Cell Transplantation, Vol. 26, pp. 115–123, 2017
Printed in the USA.

0963-6897/17 $90.00 + .00
DOI: https://doi.org/10.3727/096368916X693338
E-ISSN 1555-3892
www.cognizantcommunication.com

Effect of Gelatin on Osteogenic Cell Sheet Formation Using Canine Adipose-Derived Mesenchymal Stem Cells

Ah young Kim, Yongsun Kim, Seung Hoon Lee, Yongseok Yoon, Wan-Hee Kim, and Oh-Kyeong Kweon

BK21 PLUS Program for Creative Veterinary Science Research, Research Institute for Veterinary Science and College of Veterinary Medicine, Seoul National University, Seoul, Republic of Korea

Osteogenically differentiated cell sheet techniques using mesenchymal stem cells (MSCs) are available to stimulate bone regeneration. The advantage of the cell sheet technique is delivering live cells effectively into the focal region. We developed a novel osteogenic cell sheet technique by adding gelatin to osteogenic cell medium. Gelatin-induced osteogenic cell sheets (GCSs) were compared to conventional osteogenic cell sheets (OCSs). Undifferentiated MSCs (UCs) were used as a control. The morphology of these cell sheets was evaluated microscopically and histologically. The time-dependent cell proliferation rate was estimated by DNA quantification. The expression of osteogenic gene markers and the number of calcium depositions were assessed by quantitative real-time polymerase chain reaction and Alizarin red S (ARS) staining, respectively. GCSs were thicker and stronger than OCSs. GCSs showed a significantly higher cell proliferation rate compared to OCSs ($p<0.05$). GCSs exhibited significantly higher upregulation of BMP-7 mRNA compared to OCSs ($p<0.05$). Both GCSs and OCSs showed negative ARS reactivity on day 10, but only GCSs showed positive ARS reactivity on day 21. With this technique, we observed active cell proliferation with abundant ECM and upregulation of osteogenic bone markers, and our results suggest that GCSs could be promising for therapeutic applications in bone regeneration.

Key words: Bone regeneration; Gelatin; Mesenchymal stem cells (MSCs); Osteogenic cell sheets (OCSs)

INTRODUCTION

Cell sheet techniques have been recently developed to maximize transplanted cell survival and retention rates in vivo. The most useful advantage of cell sheet technique is delivering live cells effectively into the focal region. These techniques have been applied to several organs such as periodontal tissue, cornea, esophagus, and heart[1–3]. Additionally, osteogenically differentiated cell sheets have been applied in various ways to improve osteogenesis and bone healing: this includes direct transplantation into segmental bone defects and subcutaneous implantation in vivo[4–8].

L-Ascorbic acid 2-phosphate (Asc), a stable oxidation-resistant derivative of ascorbic acid, has been used as a supplement for producing cell sheets via stimulating extracellular matrix (ECM) production[9,10], which can easily be detached from cell culture dishes with a cell scraper. Making osteogenically differentiated cell sheets using Asc and dexamethasone (Dex) has several disadvantages such as edge folding of the cell sheet during culture[6], which implies poor-quality cell sheets. In addition, this cell matrix sheet requires at least 10 days to form the appropriate amount of matrix for in vivo applications[11].

Gelatin, a denatured collagen derived from skin tissue, has been used in many tissue-engineering applications because of its attractive characteristics of biocompatibility and biodegradability. Gelatin contains the arginine–glycine–aspartic acid (RGD) sequence, which is essential for stable relationships between the cells and the surrounding ECM[12]. The RGD sequence also enhances cell adhesion through interactions with integrin[13,14]. Therefore, gelatin, in the form of Gelfoam™, has recently been used as a scaffold material for the regeneration of tissues such as cartilage[15,16]. Pure gelatin dissolved in normal saline remains in a liquid form at 37°C. We assumed that liquefied gelatin in cell growth medium might positively affect cell proliferation and matrix formation.

We hypothesized that the addition of gelatin to cell growth medium could promote the formation of osteogenic differentiating cell matrix sheets by stimulating cell

Received September 6, 2016; final acceptance October 21, 2016. Online prepub date: October 7, 2016.
Address correspondence to Oh-Kyeong Kweon, Department of Veterinary Surgery, College of Veterinary Medicine, Seoul National University, Gwanak-ro 1, Gwanak-gu, Seoul 08826, Republic of Korea. Tel: +82-2-880-1248; Fax: +82-2-888-2866; E-mail: ohkweon@snu.ac.kr

proliferation and enhancing differentiation. The purpose of this study was to evaluate the functional properties of gelatin-induced osteogenic cell sheets (GCSs) and compare these to those of conventional osteogenic cell sheets (OCSs).

MATERIALS AND METHODS

Isolation and Cultivation of Canine Adipose-Derived Mesenchymal Stem Cells (ADSCs)

Canine ADSCs were isolated according to a procedure described in a previous report[17]. Briefly, adipose tissue was collected aseptically from subcutaneous fat of the gluteal region of 3-year-old beagle dogs. All animal experimental procedures were approved by the Institutional Animal Care and Use Committee (IACUC) of Seoul National University (SNU-141210-1) (Seoul, Republic of Korea). Approximately 1 g of adipose tissue was washed with Dulbecco's phosphate-buffered saline (DPBS; Gibco, Grand Island, NY, USA), finely minced, and digested with 1 mg/ml collagenase type I (Sigma-Aldrich, St. Louis, MO, USA) for 2 h at 37°C. The samples were washed with DPBS and then centrifuged at 980×*g* for 10 min. The stromal vascular fraction pellets were then resuspended with DPBS and filtered through a 100-μm nylon mesh. The samples were incubated overnight in low-glucose Dulbecco's modified Eagle's medium (DMEM; HyClone, Logan, UT, USA) supplemented with 10% fetal bovine serum (FBS; HyClone) in a 5% CO_2 humidified atmosphere at 37°C. The residual red blood cells and unattached cells were removed by washing with DPBS after 24 h. After achieving confluency, the cells were subcultured to 90% confluency at 48-h intervals with medium changes. Cells at passage 3 were used for experiments.

Cell Seeding and Harvesting

Mesenchymal stem cells (MSCs; 5×10^5 cells) were cultured in a 100-mm culture dish in basal medium consisting of low-glucose DMEM supplemented with 10% FBS and 1% penicillin/streptomycin (HyClone) in a 5% CO_2 humidified atmosphere. After the cells reached 70%–80% of confluency, the basal medium was replaced with a different medium according to the experimental conditions. The undifferentiated MSCs (UCs) were cultured to 100% of confluency in basal medium. The conventional OCSs were cultured in high-glucose DMEM containing 10% FBS, antibiotics, 50 μg/ml Asc (Sigma-Aldrich), and 0.1 μM Dex (Sigma-Aldrich). GCSs were cultured in high-glucose DMEM containing 10% FBS, antibiotics, 15 μg/ml Asc, 0.1 μM Dex, 10 mM β-glycerophosphate (Sigma-Aldrich), and 0.02 g/ml gelatin powder (Sigma-Aldrich). Both types of cell sheets were harvested at 1, 3, 5, 7, and 10 days of culture.

Morphological Examination and Histology

Morphological changes during cell culture were monitored and imaged using a phase-contrast microscope (Evos; Thermo Fisher Scientific, Waltham, MA, USA). OCSs and GCSs could be easily detached from culture plates. The sheets were fixed in 4% paraformaldehyde (PFA; Wako, Tokyo, Japan) for paraffin-embedded histological analysis. Sections were cut perpendicular to the cell sheet to a thickness of 5 μm, rehydrated, and stained with hematoxylin and eosin (H&E; Sigma-Aldrich).

Cell Proliferation Assay and Growth Curve

Considering the characteristics of MSC sheets, DNA quantification was selected to assess the cell proliferation rate. Canine MSCs were cultured in six-well plates in the OCS and GCS media. Total double-stranded DNA was isolated using the DNeasy Blood & Tissue Kit (Qiagen, Hilden, Germany) using the manufacturer's protocol. On days 0, 3, 5, 7, and 10, DNA content was measured using a nanophotometer (model 1443; Implen, Munich, Germany). Total DNA concentrations were proportional to total cell counts.

RNA Isolation and Real-Time Quantitative PCR

Total RNA was extracted using a Hybrid-R RNA Extraction Kit (GeneAll Biotechnology, Seoul, Republic of Korea). A single pool of complementary DNA was synthesized using a PrimeScript II First-Strand cDNA Synthesis Kit (Takara, Otsu, Japan) from 1,000 ng of total RNA as a template. Real-time polymerase chain reaction (RT-PCR) was performed using an ABI prism 7000 Sequence Detection System (Applied Biosystems, Foster, CA, USA). Ampigene quantitative (q) PCR Green Mix (Enzo Life Science, Farmingdale, NY, USA) was used to detect gene expression. The mRNA expression levels of each gene were normalized to those of glyceraldehyde 3-phosphate dehydrogenase (GAPDH) as a reference gene. Expression levels were determined with the ΔΔCt method[18]. The primer sequences of target genes are shown in Table 1 and included transforming growth factor-β (TGF-β), runt-related transcription factor 2 (Runx2), axis inhibition protein (Axin2), β-catenin, bone morphogenetic protein 7 (BMP-7), alkaline phosphatase (ALP), osteopontin (OPN), and osteocalcin (OCN). All PCR results from GCSs and OCSs were compared to those of UCs.

Alizarin Red S Staining

Samples cultured in six-well plates were washed with DPBS and fixed in 4% PFA for 10 min at room temperature (RT). Subsequently, those samples were washed with distilled water, and 2% Alizarin red S (ARS; pH 4.2) was applied to each well. The plates were then incubated for 20 min with mild shaking. After aspirating the dye, the wells were washed with distilled water[19].

Table 1. Primers for Quantitative Real-Time Polymerase Chain Reaction

	Primer Sequence (5′-3′)	
Gene	Forward	Reverse
TGF-β	CTCAGTGCCCACTGTTCCTG	TCCGTGGAGCTGAAGCAGTA
Runx2	TGTCATGGCGGGTAACGAT	TCCGGCCCACAAATCTCA
Axin2	ACGGATTCAGGCAGATGAAC	CTCAGTCTGTGCCTGGTCAA
β-Catenin	TACTGAGCCTGCCATCTGTG	ACGCAGAGGTGCATGATTTG
BMP-7	TCGTGGAGCATGACAAAGAG	GCTCCCGAATGTAGTCCTTG
ALP	TCCGAGATGGTGGAAATAGC	GGGCCAGACCAAAGATAGAG
OPN	GATGATGGAGACGATGTGGATA	TGGAATGTCAGTGGGAAAATC
OCN	CTGGTCCAGCAGATGCAAAG	GGTCAGCCAGCTCGTCACAGTT
GAPDH	CATTGCCCTCAATGACCACT	TCCTTGGAGGCCATGTAGAC

TGF-β, transforming growth factor-β; Runx2, runt-related transcription factor 2; Axin2, axis inhibition protein 2; BMP-7, bone morphogenetic protein-7; ALP, alkaline phosphatase; OPN, osteopontin; OCN, osteocalcin; GAPDH, glyceraldehyde-3-phosphate dehydrogenase.

Statistical Analysis

All measurements were analyzed by SPSS version 23.0 (IBM, Armonk, NY, USA). The Kruskal–Wallis test was used to analyze the differences between groups, and the Mann–Whitney *U*-test was used to confirm these differences. Statistically significant values were defined as $p<0.05$. Data are presented as the mean ± standard deviation (SD).

RESULTS

Morphological Changes in OCSs/GCSs

Using phase-contrast microscopy, UCs were shown to exhibit spindle-shaped morphology with clearly defined cell margins. After spindle-shaped UCs reached 70% confluency (Fig. 1A and D), the basal medium was changed to different media (OCSs or GCSs) according to the experimental schedule. Subsequently, spindle-shaped cells progressively changed to thick and cuboidal morphologies in each experimental media.

MSCs of GCSs and OCSs were attached to each other, and it was difficult to distinguish cell boundaries. The majority of cells in GCSs showed cuboidal cell shapes (Fig. 1B and E), and cells in OCSs showed a mixture of cuboidal and spindle shapes (Fig. 1C and F). After developing these cell sheet structures, OCSs and GCSs maintained their matrix form during the experimental period.

Histology of Cell Sheets

Cell sheets were easily peeled off from the culture plates using cell scrapers at day 10 of culture and were subjected to histological examination of their cross sections. H&E staining of GCSs showed three to four layers of MSCs with abundant ECM formation between the cells (Fig. 2A). Meanwhile, H&E staining of OCSs showed one to two layers of MSCs, which were thinner than those of GCSs (Fig. 2B).

Enhanced Proliferation in Gelatin Cell Sheets

The total number of cells on cell sheets was calculated proportionally from the total amount of DNA extracted from the cell sheets. DNA quantification revealed significantly higher cell proliferation in GCSs compared to OCSs, even though the number of cells seeded in each well was the same on day 0. The cell numbers were significantly increased during the first 3 days in both GCSs and OCSs compared to those on day 0 ($p<0.05$) (Fig. 3). The cell number for GCSs continued to increase steeply even after day 3, whereas that for OCSs remained constant after day 3. The cell numbers for GCSs were significantly higher than those of OCSs on each day ($p<0.05$) (Fig. 3).

The Expression of Osteogenic Markers in Cell Sheets

There was no noticeable difference in TGF-β mRNA expression between GCSs and the UCs, but upregulation of TGF-β expression was identified in OCSs after 7 days of culture ($p<0.05$) (Fig. 4A). Similarly, Runx2 mRNA expression in GCSs was not statistically different, but progressive upregulation of Runx2 was shown in OCSs from 3 days of culture, when compared to that of the UCs ($p<0.05$) (Fig. 4B). Significantly increased expression of Axin2 mRNA was observed from day 3 of culture in both GCSs and OCSs ($p<0.05$) (Fig. 4C); however, Axin2 levels were markedly higher in GCSs compared to OCSs on each day ($p<0.05$). For both GCSs and OCSs, similar trends of β-catenin mRNA upregulation were observed from day 3, when compared to that of UCs ($p<0.05$) (Fig. 4D). β-Catenin expression in GCSs peaked at day 5, whereas that in OCSs peaked at day 7. Upregulation of ALP mRNA expression in GCSs and OCSs was observed from 3 days of culture ($p<0.05$) (Fig. 4E). BMP-7 mRNA expression in GCSs and OCSs was upregulated from day 1 of culture compared to that of UCs and consistently increased thereafter. The expression of BMP-7 in GCSs

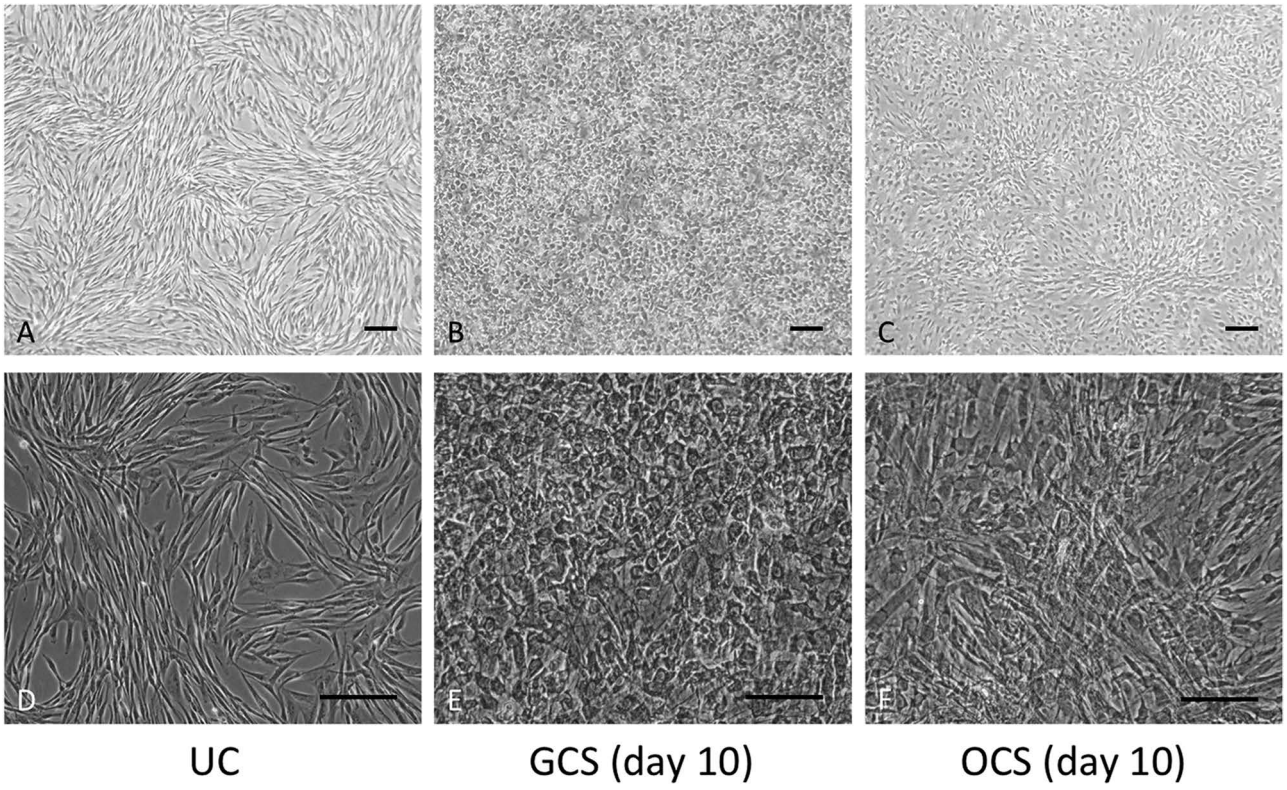

Figure 1. Morphology of canine adipose-derived mesenchymal stem cells (ADSCs) in different mediums. A phase-contrast microscope was used. Magnification: 40× (A–C), 100× (D–F). Scale bars: 200 μm. (A, D) Undifferentiated MSCs (UCs) cultured in basal medium. (B, E) Gelatin-induced osteogenic cell sheets (GCSs) cultured in basal medium containing 15 μg/ml L-ascorbic acid 2-phosphate (Asc) and 0.1 μM dexamethasone (Dex) and 0.02 g/ml gelatin powder at day 10. (C, F) Conventional osteogenic cell sheets (OCSs) cultured in basal medium containing 50 μg/ml Asc and 0.1 μM Dex at day 10.

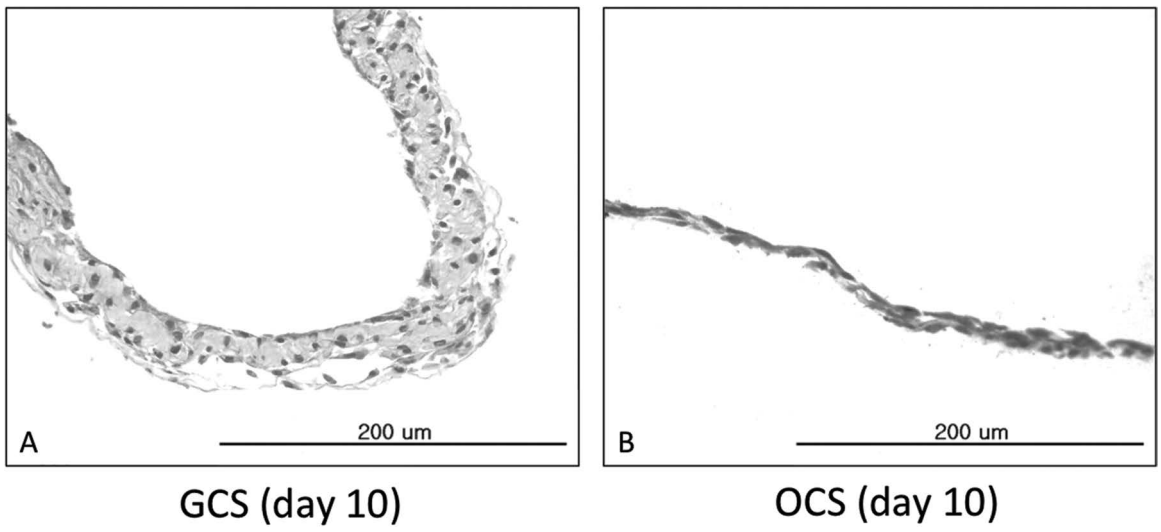

Figure 2. Hematoxylin and eosin (H&E) staining of the cross sections of gelatin-induced osteogenic cell sheets (GCSs) and conventional osteogenic cell sheets (OCSs). Scale bars: 200 μm. (A) GCS on day 10 of culture showed three to four layers of mesenchymal stem cells (MSCs) with abundant extracellular matrix (ECM). (B) OCS on day 10 of culture showed one to two layers of MSCs.

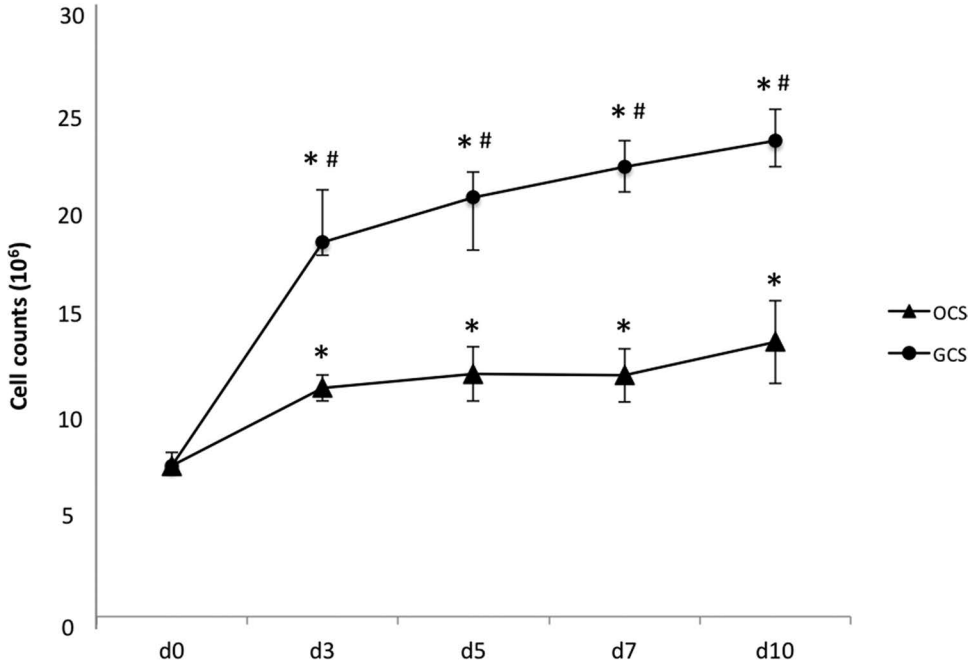

Figure 3. Cell proliferation rates on gelatin-induced osteogenic cell sheets (GCSs) and conventional osteogenic cell sheets (OCSs). The cell number for GCSs increased steeply even after day 3, whereas that for OCSs remained constant after day 3. Each point represents the mean ± standard deviation (SD). * and # a statistically significant difference compared to the cell number on day 0 and between GCSs and OCSs on each day, respectively ($p < 0.05$).

showed a steep increase at day 5, and levels from day 3 were significantly higher than those of OCSs ($p < 0.05$) (Fig. 4F). OCN expression increased from day 3 in both GCSs and OCSs ($p < 0.05$) (Fig. 4G). Expression of OPN mRNA was upregulated from day 3 in GCSs and from day 5 in OCSs, compared to that of UCs ($p < 0.05$) (Fig. 4H).

Alizarin Red S (ARS) Staining

No ARS staining was detected after 10 days of culture for either OCSs or GCSs. ARS reactivity was observed at 21 days of culture for GCSs only (Fig. 5).

DISCUSSION

A high concentration of Asc in the culture medium helps cells to form cell sheets through abundant ECM formation[6,20,21]. Previously, we studied the therapeutic application of conventional OCSs containing 50 μg/ml of Asc[11]. However, these OCSs had some drawbacks during culture periods, such as edge folding[6] and cell aggregation within the cell sheets. In addition, this strategy required at least 10 days for the formation of appropriate cell sheets for in vivo applications[11].

In the present study, GCS medium contained 15 μg/ml of Asc, which was insufficient for building cell matrix sheets. However, even with a lower concentration of Asc, GCSs showed a strong cell sheet quality. Upon histological evaluation, GCSs not only had more cell layers and a greater amount of ECM than OCSs but also showed a higher cell proliferation rate. Furthermore, the required amount of time for sheet development was shorter for GCSs. Cells in GCSs started to form a matrix sheet from day 3 of culture, but OCS cells formed a matrix sheet from day 5.

The duration of sheet formation and the thickness of the sheet depend on the number of cells and amount of ECM produced by cells. Activated Wnt signaling is associated with increased cell proliferation and the stimulation of osteogenic differentiation[22]. The Wnt pathway enhances MSC proliferation with minimal effects on the prevention of apoptosis[23]. β-Catenin and Axin2 are essential components of the canonical Wnt pathway. Axin2 negatively regulates canonical Wnt signaling by promoting β-catenin degradation and is part of a multiprotein complex containing other kinases and scaffolding proteins[24]. In GCSs, a highly upregulated Axin2 mRNA expression was shown compared to that of OCSs along with an increased β-catenin mRNA expression, which implied activated Wnt signaling. In addition, RGD peptides in gelatin stimulate cell adhesion and help proliferation of connection-dependent cells[25]. Gelatin added to the cell medium might provide MSCs with a sufficient adhesive area for cell proliferation. Significantly higher cell proliferation in GCSs seemed to be related to activated Wnt signaling and the RGD peptide sequence of gelatin.

Spindle-shaped UCs become cuboidal as they commit to the osteoblastic lineage[26]. On the basis of microscopic

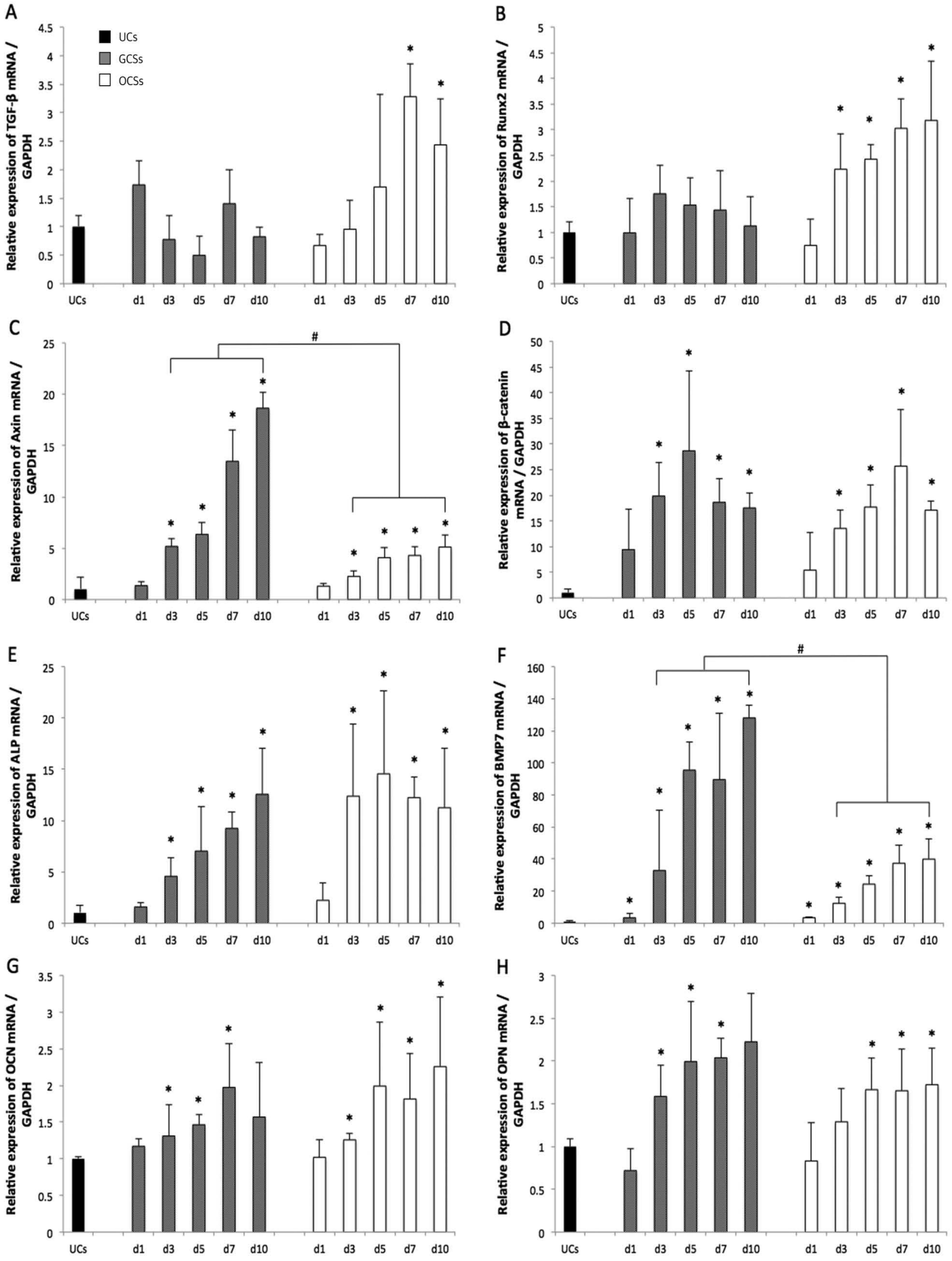
A
UCs
GCSs
OCSs
Relative expression of TGF-β mRNA / GAPDH
B
Relative expression of Runx2 mRNA / GAPDH
C
Relative expression of Axin mRNA / GAPDH
D
Relative expression of β-catenin mRNA / GAPDH
E
Relative expression of ALP mRNA / GAPDH
F
Relative expression of BMP7 mRNA / GAPDH
G
Relative expression of OCN mRNA / GAPDH
H
Relative expression of OPN mRNA / GAPDH
UCs d1 d3 d5 d7 d10 d1 d3 d5 d7 d10

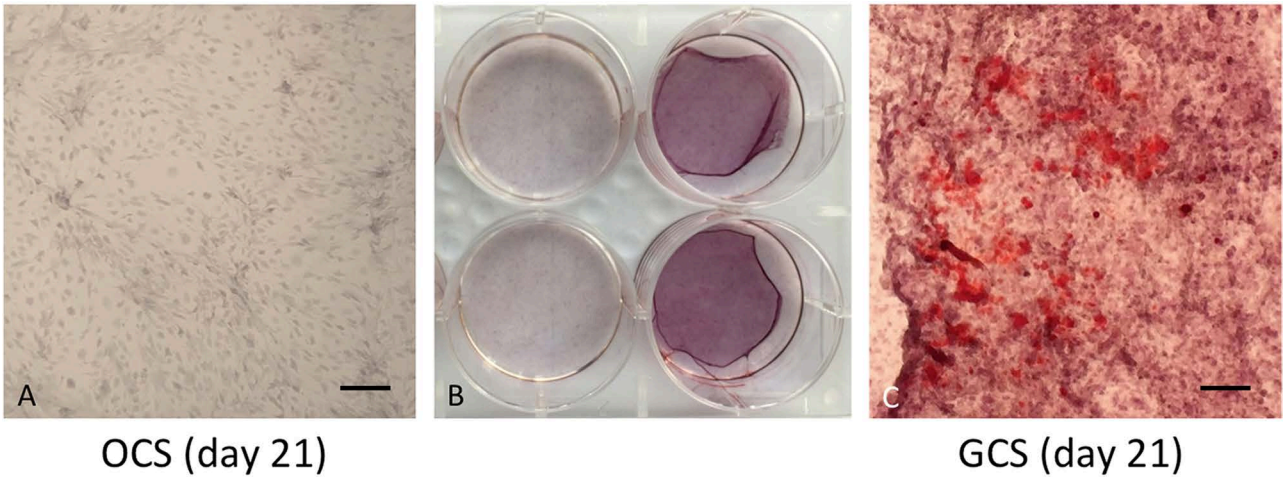

Figure 5. Alizarin red S (ARS) staining of conventional osteogenic cell sheets (OCSs) and gelatin-induced osteogenic cell sheets (GCSs) in 21 days of culture. Scale bars: 200 μm. ARS reactivity was observed only in GCSs.

evaluation at 10 days of culture, cuboidal cells were predominant in GCSs, whereas a mixture of both cuboidal and spindle cells was observed in OCSs. The changes in BMP-7 and Axin2 mRNA expression in GCSs were significantly greater than those of OCSs. Increased BMP-7 expression can indicate mature osteoblast differentiation and can promote calcium deposition[27]. Especially in relation to the significant increase in BMP-7, the proportion of osteogenically differentiated cells compared to undifferentiated cells might be higher in GCSs than in OCSs.

Osteogenesis consists of three phases including osteogenitor proliferation, matrix maturation, and matrix mineralization[28]. During the early stage of bone formation, the coordination of Runx2 and BMP/TGF-β signaling is important and can induce osteoprogenitor proliferation and stimulate uncommitted progenitors to differentiate into osteoblasts[29,30]. The functions of Runx2 include directing MSCs to an osteoblast lineage and stimulating the expression of bone matrix protein genes such as ALP[31]. Osteopontin is another early osteogenic marker[32].

In OCSs, Runx2 expression was upregulated from day 3, followed by the upregulation of TGF-β from day 5. BMP-7 and ALP expression levels were upregulated from days 1 and 3, respectively, and thereafter constantly increased. In GCSs however, the expression levels of Runx2 and TGF-β remained relatively low compared to those of OCSs, even though ALP and BMP-7 expression levels progressively increased. This suggested that MSCs in GCS and OCS media might have induced different pathways to become osteogenically differentiated cell sheets.

The canonical Wnt/β-catenin pathway is another essential signaling pathway for bone regulatory events such as bone formation, remodeling, and osteoblastic differentiation[33]. The relationship between Wnt signaling and osteogenic differentiation in MSCs is controversial. Wnt/β-catenin activity has been reported to commit mouse MSCs into an osteoblastic lineage[34,35]. However, some studies have observed that the canonical Wnt pathway has both stimulatory[36] and inhibitory[37] effects on the osteogenic differentiation of MSCs.

β-Catenin mRNA expression in GCSs and OCSs was similarly upregulated, but Axin2 mRNA expression was different. Even though both GCSs and OCSs had significantly increased Axin2 expression levels compared to the control, the levels in GCSs were substantially higher compared to those of OCSs. This result implies that Wnt/β-catenin signaling was activated more so in GCSs. Considering overall osteogenic marker expression levels, osteogenic differentiation in GCSs could be

FACING PAGE

Figure 4. Osteogenic gene marker expression profiles of undifferentiated mesenchymal stem cells (UCs; black color), gelatin-induced osteogenic cell sheets (GCSs; gray color), and conventional osteogenic cell sheets (OCSs; white color) at 1, 3, 5, 7, and 10 days. Serial mRNA expressions relative to glyceraldehyde 3-phosphate dehydrogenase (GAPDH) were evaluated using quantitative real-time polymerase chain reaction (RT-PCR) for (A) transforming growth factor-β (TGF-β), (B) runt-related transcription factor 2 (Runx2), (C) axis inhibition protein 2 (Axin2), (D) β-catenin, (E) alkaline phosphatase (ALP), (F) bone morphogenetic protein-7 (BMP-7), (G) osteocalcin (OCN), and (H) osteopontin (OPN). Each bar shows the mean ± standard deviation (SD). * and # a statistically significant difference compared to UCs, and between GCSs and OCSs on each day, respectively ($p < 0.05$).

attributed to Wnt/β-catenin signaling rather than Runx2/TGF-β signaling.

Osteocalcin is a late bone-related marker that is only secreted by mature osteoblasts and indicates terminal osteoblast differentiation[38]. In both GCSs and OCSs, upregulations of osteocalcin were observed compared to UCs. After maturation of the ECM, mineralization follows via the deposition of calcium and phosphate[39]. Mineral depositions in both types of sheets, at day 10, were insufficient to be stained by ARS; however, ARS reactivity was observed after further culture of GCSs, specifically at day 21. Cells in both types of sheets after 10 days of culture might differentiate into the matrix maturation phase, which precedes the matrix mineralization phase.

Though Runx2 induces early osteoprogenitor differentiation and proliferation, it inhibits the mineralization of osteoblasts in the later phase of osteogenesis[31]. The Runx2 expression level of GCSs was similar to that of UCs, while the level of OCSs was significantly increased from day 3 of culture. Cells in GCS medium might have less exposure to Runx2 signals than cells in OCS medium, which can promote the mineralization in GCSs. Therefore, the different degree of mineralization between the two sheets seemed to be related with the level of expression of Runx2.

BMP-7 expression in GCSs was particularly high, compared to that of OCSs, and ARS reactivity was observed only in GCSs. These results imply that the osteogenicity of GCSs might be superior to that of OCSs. The results of this study indicate that the addition of gelatin to the osteogenic medium has positive effects on early cell matrix formation and induces a high level of cell proliferation and an outstanding osteogenic differentiation program in MSCs through the activation of the Wnt pathway and interaction with RGD sequences. Another report also showed that RGD peptides could accelerate osteoblast proliferation and bone formation[40].

GCSs exhibited superior osteogenic transdifferentiation capabilities and a remarkable cell proliferation rate, compared to those of conventional OCSs. With this method, we could overcome the drawbacks of OCSs, including their relatively weak cell sheet quality. In addition, we observed that GCSs have a stronger matrix compared to OCSs, which is an important advantage for in vivo applications. Our results prove that GCSs are promising for bone regeneration applications.

ACKNOWLEDGMENTS: This research was supported by the National Research Foundation of Korea (NRF-2013R1A1A2004506). The authors declare no conflict of interests.

REFERENCES

1. Sekine H, Shimizu T, Dobashi I, Matsuura K, Hagiwara N, Takahashi M, Kobayashi E, Yamato M, Okano T. Cardiac cell sheet transplantation improves damaged heart function via superior cell survival in comparison with dissociated cell injection. Tissue Eng Part A 2011;17(23–24):2973–80.
2. Sumide T, Nishida K, Yamato M, Ide T, Hayashida Y, Watanabe K, Yang J, Kohno C, Kikuchi A, Maeda N, Watanabe H, Okano T, Tano Y. Functional human corneal endothelial cell sheets harvested from temperature-responsive culture surfaces. FASEB J. 2006;20(2):392–4.
3. Yang J, Yamato M, Shimizu T, Sekine H, Ohashi K, Kanzaki M, Ohki T, Nishida K, Okano T. Reconstruction of functional tissues with cell sheet engineering. Biomaterials 2007;28(34):5033–43.
4. Nakamura A, Akahane M, Shigematsu H, Tadokoro M, Morita Y, Ohgushi H, Dohi Y, Imamura T, Tanaka Y. Cell sheet transplantation of cultured mesenchymal stem cells enhances bone formation in a rat nonunion model. Bone 2010;46(2):418–24.
5. Inagaki Y, Uematsu K, Akahane M, Morita Y, Ogawa M, Ueha T, Shimizu T, Kura T, Kawate K, Tanaka Y. Osteogenic matrix cell sheet transplantation enhances early tendon graft to bone tunnel healing in rabbits. Biomed Res Int. 2013;2013:842192.
6. Guo P, Zeng JJ, Zhou N. A novel experimental study on the fabrication and biological characteristics of canine bone marrow mesenchymal stem cells sheet using vitamin C. Scanning 2015;37(1):42–8.
7. Akahane M, Nakamura A, Ohgushi H, Shigematsu H, Dohi Y, Takakura Y. Osteogenic matrix sheet-cell transplantation using osteoblastic cell sheet resulted in bone formation without scaffold at an ectopic site. J Tissue Eng Regen Med. 2008;2(4):196–201.
8. Kim Y, Lee SH, Kang BJ, Kim WH, Yun HS, Kweon OK. Comparison of osteogenesis between adipose derived mesenchymal stem cells and their sheets on poly-epsilon-caprolactone/beta-tricalcium phosphate composite scaffolds in canine bone defects. Stem Cells Int. 2016;2016:8414715.
9. Kim JE, Jin DH, Lee SD, Hong SW, Shin JS, Lee SK, Jung DJ, Kang JS, Lee WJ. Vitamin C inhibits p53-induced replicative senescence through suppression of ROS production and p38 MAPK activity. Int J Mol Med. 2008;22(5):651–5.
10. Taniguchi M, Arai N, Kohno K, Ushio S, Fukuda S. Antioxidative and anti-aging activities of 2-O-alpha-glucopyranosyl-L-ascorbic acid on human dermal fibroblasts. Eur J Pharmacol. 2012;674(2–3):126–31.
11. Kuk M, Kim Y, Lee SH, Kim WH, Kweon OK. Osteogenic ability of canine adipose derived mesenchymal stromal cell sheets in relation to culture time. Cell Transplant. 2016;25(7):1415–22.
12. Hoch E, Schuh C, Hirth T, Tovar GE, Borchers K. Stiff gelatin hydrogels can be photo-chemically synthesized from low viscous gelatin solutions using molecularly functionalized gelatin with a high degree of methacrylation. J Mater Sci Mater Med. 2012;23(11):2607–17.
13. Wu SC, Chang WH, Dong GC, Chen KY, Chen YS, Yao CH. Cell adhesion and proliferation enhancement by gelatin nanofiber scaffolds. J Bioact Compat Polym. 2011;26(6):565–577.
14. Rosellini E, Cristallini C, Barbani N, Vozzi G, Giusti P. Preparation and characterization of alginate/gelatin blend films for cardiac tissue engineering. J Biomed Mater Res A 2009;91(2):447–53.
15. Ponticiello MS, Schinagl RM, Kadiyala S, Barry FP. Gelatin-based resorbable sponge as a carrier matrix for

human mesenchymal stem cells in cartilage regeneration therapy. J Biomed Mater Res. 2000;52(2):246–55.
16. Pesakova V, Stol M, Adam M. Comparison of the influence of gelatine and collagen substrates on growth of chondrocytes. Folia Biol. (Praha) 1990;36(5):264–70.
17. Ryu HH, Lim JH, Byeon YE, Park JR, Seo MS, Lee YW, Kim WH, Kang KS, Kweon OK. Functional recovery and neural differentiation after transplantation of allogenic adipose-derived stem cells in a canine model of acute spinal cord injury. J Vet Sci. 2009;10(4):273–84.
18. Livak KJ, Schmittgen TD. Analysis of relative gene expression data using real-time quantitative PCR and the 2(-Delta Delta C(T)) method. Methods 2001;25(4):402–8.
19. Gregory CA, Gunn WG, Peister A, Prockop DJ. An Alizarin red-based assay of mineralization by adherent cells in culture: Comparison with cetylpyridinium chloride extraction. Anal Biochem. 2004;329(1):77–84.
20. Wei F, Qu C, Song T, Ding G, Fan Z, Liu D, Liu Y, Zhang C, Shi S, Wang S. Vitamin C treatment promotes mesenchymal stem cell sheet formation and tissue regeneration by elevating telomerase activity. J Cell Physiol. 2012; 227(9):3216–24.
21. Yu J, Tu YK, Tang YB, Cheng NC. Stemness and transdifferentiation of adipose-derived stem cells using L-ascorbic acid 2-phosphate-induced cell sheet formation. Biomaterials 2014;35(11):3516–26.
22. Liu G, Vijayakumar S, Grumolato L, Arroyave R, Qiao H, Akiri G, Aaronson SA. Canonical Wnts function as potent regulators of osteogenesis by human mesenchymal stem cells. J Cell Biol. 2009;185(1):67–75.
23. Dravid G, Ye Z, Hammond H, Chen G, Pyle A, Donovan P, Yu X, Cheng L. Defining the role of Wnt/beta-catenin signaling in the survival, proliferation, and self-renewal of human embryonic stem cells. Stem Cells 2005;23(10): 1489–501.
24. Yan Y, Tang D, Chen M, Huang J, Xie R, Jonason JH, Tan X, Hou W, Reynolds D, Hsu W, Harris SE, Puzas JE, Awad H, O'Keefe RJ, Boyce BF, Chen D. Axin2 controls bone remodeling through the beta-catenin-BMP signaling pathway in adult mice. J Cell Sci. 2009;122(Pt 19):3566–78.
25. Hersel U, Dahmen C, Kessler H. RGD modified polymers: Biomaterials for stimulated cell adhesion and beyond. Biomaterials 2003;24(24):4385–415.
26. Zhang Y, Khan D, Delling J, Tobiasch E. Mechanisms underlying the osteo- and adipo-differentiation of human mesenchymal stem cells. ScientificWorldJournal 2012;2012: 793823.
27. Shen B, Wei A, Whittaker S, Williams LA, Tao H, Ma DD, Diwan AD. The role of BMP-7 in chondrogenic and osteogenic differentiation of human bone marrow multipotent mesenchymal stromal cells in vitro. J Cell Biochem. 2010;109(2):406–16.
28. Owen TA, Aronow M, Shalhoub V, Barone LM, Wilming L, Tassinari MS, Kennedy MB, Pockwinse S, Lian JB, Stein GS. Progressive development of the rat osteoblast phenotype in vitro: Reciprocal relationships in expression of genes associated with osteoblast proliferation and differentiation during formation of the bone extracellular matrix. J Cell Physiol. 1990;143(3):420–30.
29. Komori T. Regulation of skeletal development by the Runx family of transcription factors. J Cell Biochem. 2005; 95(3):445–53.
30. Chen G, Deng C, Li YP. TGF-beta and BMP signaling in osteoblast differentiation and bone formation. Int J Biol Sci. 2012;8(2):272–88.
31. Komori T. Regulation of osteoblast differentiation by transcription factors. J Cell Biochem. 2006;99(5):1233–9.
32. Huang JI, Beanes SR, Zhu M, Lorenz HP, Hedrick MH, Benhaim P. Rat extramedullary adipose tissue as a source of osteochondrogenic progenitor cells. Plast Reconstr Surg. 2002;109(3):1033–41; discussion 1042–3.
33. Zhang JF, Li G, Chan CY, Meng CL, Lin MC, Chen YC, He ML, Leung PC, Kung HF. Flavonoids of Herba Epimedii regulate osteogenesis of human mesenchymal stem cells through BMP and Wnt/beta-catenin signaling pathway. Mol Cell Endocrinol. 2010;314(1):70–4.
34. Gaur T, Lengner CJ, Hovhannisyan H, Bhat RA, Bodine PV, Komm BS, Javed A, van Wijnen AJ, Stein JL, Stein GS, Lian JB. Canonical WNT signaling promotes osteogenesis by directly stimulating Runx2 gene expression. J Biol Chem. 2005;280(39):33132–40.
35. Gong Y, Slee RB, Fukai N, Rawadi G, Roman-Roman S, Reginato AM, Wang H, Cundy T, Glorieux FH, Lev D, Zacharin M, Oexle K, Marcelino J, Suwairi W, Heeger S, Sabatakos G, Apte S, Adkins WN, Allgrove J, Arslan-Kirchner M, Batch JA, Beighton P, Black GC, Boles RG, Boon LM, Borrone C, Brunner HG, Carle GF, Dallapiccola B, De Paepe A, Floege B, Halfhide ML, Hall B, Hennekam RC, Hirose T, Jans A, Jüppner H, Kim CA, Keppler-Noreuil K, Kohlschuetter A, LaCombe D, Lambert M, Lemyre E, Letteboer T, Peltonen L, Ramesar RS, Romanengo M, Somer H, Steichen-Gersdorf E, Steinmann B, Sullivan B, Superti-Furga A, Swoboda W, van den Boogaard MJ, Van Hul W, Vikkula M, Votruba M, Zabel B, Garcia T, Baron R, Olsen BR, Warman ML; Osteoporosis-Pseudoglioma Syndrome Collaborative Group. LDL receptor-related protein 5 (LRP5) affects bone accrual and eye development. Cell 2001;107(4):513–23.
36. Gregory CA, Gunn WG, Reyes E, Smolarz AJ, Munoz J, Spees JL, Prockop DJ. How Wnt signaling affects bone repair by mesenchymal stem cells from the bone marrow. Ann N Y Acad Sci. 2005;1049:97–106.
37. Boland GM, Perkins G, Hall DJ, Tuan RS. Wnt 3a promotes proliferation and suppresses osteogenic differentiation of adult human mesenchymal stem cells. J Cell Biochem. 2004;93(6):1210–30.
38. Tracy RP, Andrianorivo A, Riggs BL, Mann KG. Comparison of monoclonal and polyclonal antibody-based immunoassays for osteocalcin: A study of sources of variation in assay results. J Bone Miner Res. 1990;5(5):451–61.
39. Park BW, Hah YS, Kim DR, Kim JR, Byun JH. Osteogenic phenotypes and mineralization of cultured human periosteal-derived cells. Arch Oral Biol. 2007;52(10):983–9.
40. Kantlehner M, Schaffner P, Finsinger D, Meyer J, Jonczyk A, Diefenbach B, Nies B, Holzemann G, Goodman SL, Kessler H. Surface coating with cyclic RGD peptides stimulates osteoblast adhesion and proliferation as well as bone formation. Chembiochem. 2000;1(2):107–14.